Clean and polluted clouds: Relationships among pollution, ice clouds, and precipitation in South America

Jonathan H. Jiang,[1] Hui Su,[1] Mark R. Schoeberl,[2] Steven T. Massie,[3] Peter Colarco,[2] Steven Platnick,[2] and Nathaniel J. Livesey[1]

Received 8 May 2008; accepted 16 June 2008; published 17 July 2008.

[1] We analyze nearly-simultaneous measurements of ice clouds and pollutants along satellite tracks. We use Aura MLS CO and ice water content measurements at 215 hPa to classify ice clouds as "clean" or "polluted". We then examine Aqua MODIS ice particle effective radius (r_e) and aerosol optical thickness (AOT) along with TRMM precipitation to investigate how pollution changes ice particle size and precipitation. We find suppressed precipitation and reduced r_e associated with polluted clouds during the dry season in South America when there is a strong positive correlation between the CO and AOT. In contrast, during the wet season, we find little difference in ice particle size and precipitation between the polluted clouds and the clean clouds, as indicated by the CO levels, when the AOT is significantly lower than that in the dry season. **Citation:** Jiang, J. H., H. Su, M. R. Schoeberl, S. T. Massie, P. Colarco, S. Platnick, and N. J. Livesey (2008), Clean and polluted clouds: Relationships among pollution, ice clouds, and precipitation in South America, *Geophys. Res. Lett.*, *35*, L14804, doi:10.1029/2008GL034631.

1. Introduction

[2] Aerosol pollutants provide a source of cloud condensation nuclei (CCN) and thus can have a considerable impact on climate through alternation of cloud microphysical properties and related changes in precipitation [*Lohmann and Feichter*, 2005]. There is still great uncertainty in the magnitude of the so-called "indirect" effect of aerosols [*Intergovernmental Panel on Climate Change*, 2007], which has the potential to substantially offset the positive forcing due to greenhouse gases [*Penner et al.*, 2001]. In the case of low-level liquid clouds, two likely indirect effects of aerosols have been theorized. For a fixed liquid water content (LWC), the *first* indirect effect is a decrease in average cloud droplet size (effective radius) when aerosol loading leads to an increase of the cloud droplet number concentration [*Twomey*, 1977]. The smaller cloud droplet size leads to a change in the cloud albedo, making clouds brighter [*Twomey et al.*, 1984; *Facchini et al.*, 1999]. The *second* indirect effect is the suppression of raindrop development since the collision efficiency is weaker for smaller droplets. This leads to a decrease in precipitation efficiency and extends the cloud lifetime [*Albrecht*, 1989; *Ramanathan et al.*, 2001]. General circulation model (GCM) simulated global annual mean radiative perturbations due to the aerosol indirect effect at the top of atmosphere (TOA) are in the range of -0.3 to -1.4 Wm^{-2} due to changes in cloud lifetime, and -0.5 to -1.9 Wm^{-2} due to changes in cloud albedo [*Lohmann and Feichter*, 2005].

[3] There are many observational studies that have studied aerosol indirect effects on low-level clouds [e.g., *Kaufman and Fraser*, 1997; *Nakajima et al.*, 2001; *Coakley and Walsh*, 2002; *Sekiguchi et al.*, 2003; *Matheson et al.*, 2005]. However, estimates of the aerosol-cloud interaction on precipitation have been difficult to make and the few observational studies have shown conflicting results. For example, using Tropical Rainfall Measuring Mission (TRMM) observations, *Rosenfeld* [1999] shows that aerosol emissions from vegetation fires may lead to a decrease or total shutoff of convective precipitation. On the other hand, by examining relationships of aerosol optical thickness (AOT) measured from the Moderate Resolution Imaging Spectroradiometer (MODIS) versus TRMM rainfall over the Amazon during biomass burning seasons of 2000 and 2003, *Lin et al.* [2006] found increased rainfall associated with elevated AOT.

[4] While the influence of aerosols on liquid cloud has received considerable attention, the connection between aerosols and ice cloud remains largely unknown [*Penner et al.*, 2001]. GCM simulations of indirect effect of aerosols on ice clouds have been very limited. On the observational front, analyses of ISCCP data by *Sherwood* [2002] indicated that the effective radius of ice particles at the top of tropical cumulonimbus decreases in regions where the Total Ozone Mapping Spectrometer (TOMS) aerosol index is high. Sherwood therefore suggested that aerosols reduce cloud base liquid droplet size. The smaller liquid droplets become frozen as they are lofted, replicating the altered cloud base particle distribution in the deep convective cloud tops and associated anvil outflow. In contrast to *Sherwood*'s [2002] results, the analyses of *Chylek et al.* [2006] and *Massie et al.* [2007] did not support a decrease in cloud particle size as aerosol increases. *Chylek et al.* [2006] used MODIS data and found that ice particles during winter over the Indian Ocean are shifted towards larger sizes during the episodes of increased regional pollution. *Massie et al.* [2007] also studied MODIS aerosol and radiances over the Indian Ocean, and concluded that liquid droplets exhibited the expected decrease in size with an increase in aerosol optical depth, while ice particles exhibited little change in size. At least some of these differences in the previous studies may result from differences in geographical regions, time periods, samples of clouds, as well as analysis methodologies.

[1] Jet Propulsion Laboratory, California Institute of Technology, Pasadena, California, USA.
[2] NASA Goddard Space Flight Center, Greenbelt, Maryland, USA.
[3] National Center for Atmospheric Research, Boulder, Colorado, USA.

0094-8276/08/2008GL034631

[5] In this study we analyze nearly-simultaneous observations along the Aura Microwave Limb Sounder (MLS) tracks to study relationships among pollutants, ice clouds and precipitation. We use MLS CO measurements as a proxy of pollution to classify ice clouds observed by MLS as "clean" or "polluted". The validity of this CO as a proxy of aerosol is tested by correlations between the CO and Aqua MODIS AOT data that are interpolated onto MLS measurement locations. Since MLS IWC and CO are simultaneous retrievals, it is more convenient to use CO to classify "polluted" and "clean" clouds rather than interpolated aerosol measurements from Aqua MODIS. The use of MLS CO-IWC pairs maximizes the number of samples in cloudy regions where the AOT data have many missing values. We shall see later that CO is only a good aerosol proxy in some cases but not always good in others, which enriches our perspectives to study the interaction of aerosol, clouds and precipitation. We interpolate Aqua MODIS ice particle effective radius (r_e) and TRMM precipitation data onto MLS measurement locations to investigate the differences in r_e and precipitation associated with clean and polluted clouds. We also interpolate NCEP vertical velocity and boundary layer divergence onto MLS tracks to study differences in dynamical conditions for clean and polluted clouds. Our analyses focus on the South America region, where reduction of droplet sizes in low-level warm clouds has been observed with an increase of aerosols due to biomass burning [e.g., *Kaufman and Fraser*, 1997; *Andreae et al.*, 2004].

2. Data

2.1. Aura MLS

[6] We use Aura MLS Level 2 CO and IWC measurements (V2.2) from 1 September, 2004 to 31 December 2007. The CO is retrieved from the 230 GHz emission line, and the IWC is retrieved from the cloud-induced radiance at 240 GHz. The retrieval methods and validation of MLS CO and IWC products are described by *Livesey et al.* [2008] and *Wu et al.* [2008], respectively. For this study, the CO and IWC data at 215 hPa ($\sim$11 km) are used. This altitude is the lowest upper tropospheric level where MLS CO retrievals are available; it is also close to the level of maximum convective detrainment [*Folkins and Martin*, 2005]. At 215 hPa, the along track horizontal resolution is about 300 km for IWC and 500 km for CO, and the vertical resolution is about 4 km for IWC and 5 km for CO. The estimated single measurement precisions are $\sim$20% for CO and $\sim$1 mg/m^3 for IWC. Although the morphology of MLS CO has been validated to be realistic, there is a known factor-of-2 high bias in the CO value at 215 hPa. Since this study focuses on the correlation between relevant parameters, rather than the absolute values, the high CO bias does not affect our analysis results.

2.2. Aqua MODIS

[7] The AOT daily data used in this study are generated from the Aqua MODIS Level 2 aerosol product (MYD04). The AOT properties are derived by inversion of observed reflectance at 500 m resolution using computed radiative transfer parameters based on a dynamical aerosol model of *Kaufman et al.* [1997]. The accuracies of the AOT (τ) are $\Delta\tau = \pm 0.03 \pm 0.05\tau$ over ocean and $\Delta\tau = \pm 0.05 \pm 0.15\tau$ over land [*Remer et al.*, 2005]. The AOT data are aggregated to 1° latitude by 1.25° longitude grids.

[8] The Aqua MODIS daily aggregation of ice cloud effective radius r_e is obtained from the Collection 005 Level-3 MOD08-D3 product. The retrieval of r_e is based on the spectral signature of reflected radiation from clouds that varies with the cloud particle size [*Nakajima and King*, 1990; *Platnick et al.*, 2003]. With MODIS measurements from two wavelengths, r_e and cloud optical thickness can be retrieved from a pre-computed look up table of reflectances that span the retrieval space. One measurement is at a non-absorbing wavelength (channel) having minimum surface contribution (e.g., 0.65 μm over land and 0.86 μm over the ocean). Another set of measurements in cloud water absorbing channels at 1.6, 2.1, and 3.7 μm are selected to probe different cloud vertical depths. For a given cloud optical thickness, cloud reflectance in the absorbing channels decrease as the particle size increases. The Level-3 MOD08_D3 cloud optical and microphysical products are generated by sub-sampling every fifth pixel of the 1 km Level-2 swath product (MYD06). The data are binned at a $1° \times 1°$ resolution. The MYD06 product includes baseline uncertainties for r_e as well as other retrieved quantities; for ice clouds these can be quite variable depending on the corresponding cloud optical thickness and solar/viewing geometry, but are typically in the 10% range. The valid retrieval range for ice cloud r_e is 5–90 μm.

2.3. TRMM

[9] We use TRMM precipitation data (3B42) [*Huffman et al.*, 2001]. The data have 3-hour temporal resolution and $0.25° \times 0.25°$ spatial resolution in a global belt from 50°S to 50°N. The TRMM 3B42 products combine both microwave and infrared measurements, and also include gauge data to give the best estimate of precipitation. There are two known deficiencies of the data: The infrared data prior to February 2002 covers only 40°S to 40°N, after that the data covers 50°S and 50°N; and there is a 10% likely low bias caused by introduction of AMSU-B data after 2002.

2.4. NCEP

[10] The 6-hourly 500 hPa vertical wind data from the NCEP reanalysis are used. We also computed the divergence at 850 hPa from NCEP 6-hourly horizontal u, v winds.

2.5. Data Collocation

[11] In order to have collocated datasets, the 3-hourly TRMM precipitation and 6-hourly NCEP vertical winds and divergence data are interpolated onto the MLS measurement locations in both space and time. The Aura and Aqua satellites belong to the "A-Train" family [*Schoeberl and Talabac*, 2007] and are both polar-orbiting satellites with equatorial crossing times of $\sim$1:30 am (descending orbits) and 1:30 pm (ascending orbits). The MLS measurements are behind MODIS observations by less than 10 minutes and thus we consider them near-simultaneous. The daily MODIS r_e and AOT data are sampled onto the MLS measurement locations by using the nearest MODIS data for each MLS data point. We also screen the data according

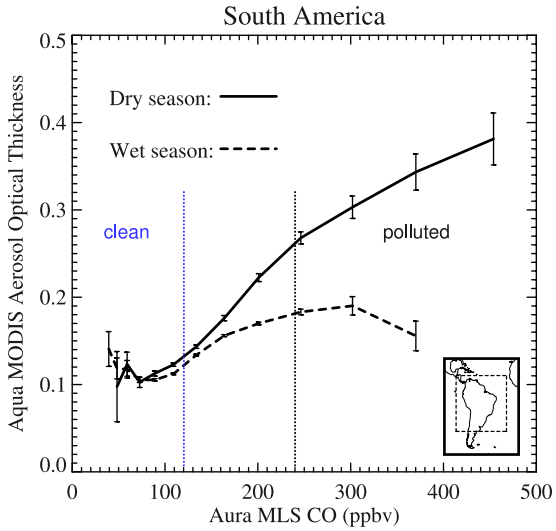

Figure 1. Aqua MODIS AOT binned on the collocated Aura MLS CO at 215 mb for both the dry, biomass burning period (June–October) and the wet, rainy period (November–May). All of the MLS and MODIS collocated measurements within the dash-line box in the geographical inset are used, which covers all the dry and wet periods between September 2004 and December 2007. The error bars in Figures 1–3 denote the standard errors ($\sigma/\sqrt{N}$) of the bin average.

to both MLS and MODIS data quality requirements to ensure the best quality of the collocated datasets.

3. Results

[12] We first use the simultaneous measurements of CO and IWC from Aura MLS to distinguish "polluted" clouds from "clean" clouds. CO is produced by fossil-fuel (e.g., coal, petroleum) and biomass (e.g., forest) burning. It is not water soluble and has a longer lifetime (about 2 months) than aerosols. High values of CO in the upper troposphere are usually associated with pollution uplifted by convection [e.g., *Jiang et al.*, 2007]. Thus convective clouds that are contaminated by aerosols usually also exhibit high values of CO. Figure 1 shows Aura MLS CO versus Aqua MODIS AOT over South America. The AOT data are binned according to the collocated MLS CO at 215 hPa for both the dry, biomass burning period (June–October) and the wet, rainy period (November–May). All the MLS and MODIS collocated measurements within the dashed-line box over the South America region (as indicated in the inset) are used, which span September 2004 to December 2007. During the dry period, CO is positively correlated with the AOT, suggesting enhanced CO can be used as a proxy of aerosol loading. During the wet season, the AOT is significantly lower than that in the dry season, possibly because of lower source emissions [*Artaxo et al.*, 2002] and frequent precipitation that washes out aerosols. The CO can still be quite high, due to the longer lifetime of CO relative to aerosol and due to the transport of CO from other regions.

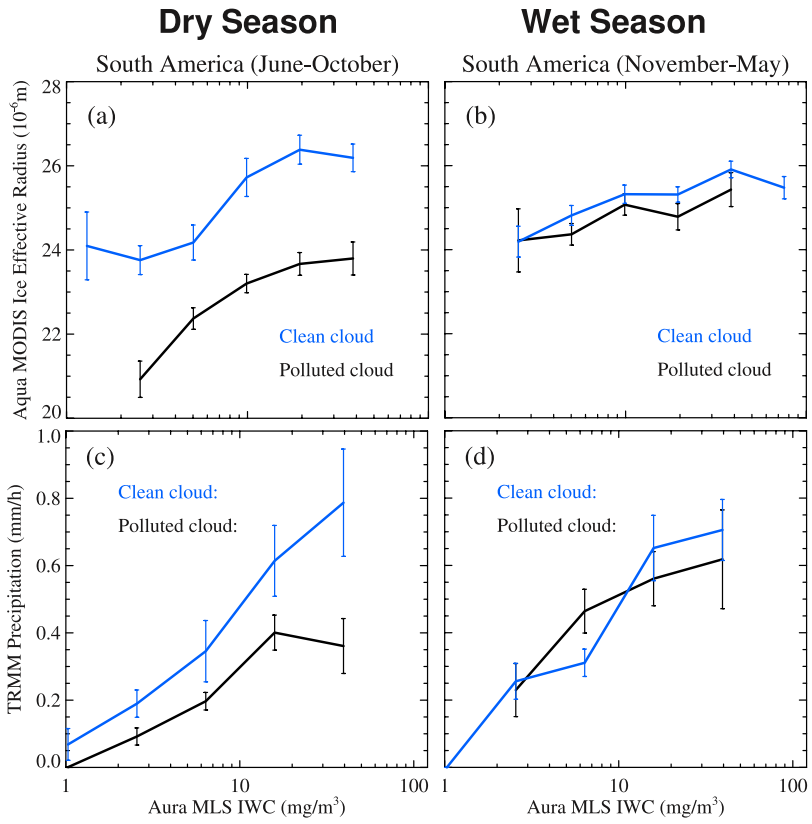

Figure 2. (a) Aqua MODIS ice cloud effective radius data binned according to the collocated MLS IWCs for clean and polluted clouds during dry season; (b) same as Figure 2a but for wet season; (c) TRMM precipitation data binned on the collocated MLS IWC for clean and polluted clouds during the dry season; (d) same as Figure 2c but for wet season.

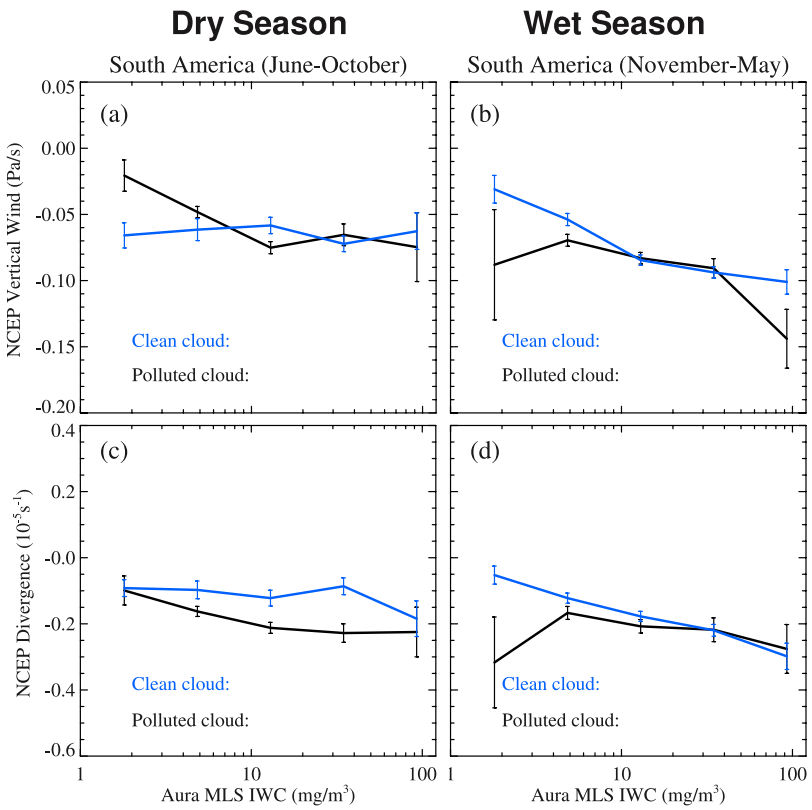

Figure 3. (a and c) NCEP 500 hPa vertical winds and 850 hPa divergence binned according to the collocated MLS IWCs for clean and polluted clouds during dry season; (b and d) same as Figures 3a and 3c but for wet season.

[13] We separate "clean" clouds from "polluted" clouds in the following manner: for each MLS measurement along the track at 215 hPa, the "clean" cloud IWC is defined by the collocated CO value < 120 ppbv; the "polluted" cloud IWC is defined by the collocated CO value > 240 ppbv. We choose the low and high ends of CO values to achieve distinct signals for the clean and polluted cases. We then use the collocated MODIS data to investigate how the ice particle sizes and associated precipitation changes are related with the polluted and clean clouds. Figures 2a and 2b show the MODIS ice cloud effective radii (r_e) binned according to the collocated MLS clean/polluted cloud IWCs for the dry and wet seasons of South America, respectively. In general, larger IWC values are associated with larger cloud particles. The polluted clouds are associated with smaller particles than that of the clean clouds, especially during the dry biomass burning season when the aerosol concentration is relatively high. Figures 2c and 2d show the relationship between the collocated TRMM precipitation and MLS IWC for clean/polluted clouds during the dry and wet seasons. During the dry season, polluted clouds are associated with weaker precipitation than clean clouds. The rainfall difference between polluted and clean clouds is much smaller during the wet season.

[14] Since surface precipitation is governed by many dynamical and thermodynamical factors as well as aerosol impact, we examined a number of variables that might contribute to the different precipitation values for polluted/clean clouds and for the wet/dry seasons. Figure 3 shows the collocated NCEP 500 hPa vertical velocity and 850 hPa wind divergence binned on MLS IWC at 215 hPa for clean/polluted clouds and wet/dry seasons. We find that both the clean and polluted clouds are generally associated with upward vertical winds in the mid-troposphere (500 hPa) and horizontal convergence of air in the boundary layer (850 hPa). The magnitudes of vertical velocities are quite similar for clean and polluted clouds during both seasons. During the dry season, the 850 hPa convergence is stronger for polluted clouds than for clean clouds. This is in line with *Andreae et al.* [2004], who also found a stronger updraft in polluted convective liquid water clouds. This, however, can not explain the weaker precipitation associated with polluted clouds. During the wet season, the difference in convergence for polluted and clean clouds is quite small.

[15] Given that the difference in vertical winds and boundary layer convergence cannot explain the precipitation differences for clean and polluted clouds, we think the reduced precipitation for polluted clouds is mainly a manifestation of interactions between aerosol and precipitation. Several effects can be active. One is aerosol scavenging by raindrops and wet deposition, in that stronger precipitation is usually associated with less aerosol particles. Another is the microphysical effect of aerosol on clouds, through reducing cloud particle size and thus precipitation efficiency.

The change of radiative heating due to aerosol direct radiative forcing and cloud-radiation interactions may also contribute to the precipitation changes. The exact mechanisms can not be identified directly from the observations here. Nevertheless, our analysis presents the first-order relationships among aerosol, ice clouds and precipitation, which can guide further modeling studies to understand the causality.

4. Conclusion

[16] We analyzed collocated satellite measurements of Aura MLS CO, IWC, Aqua MODIS AOT, ice cloud effective radius, and TRMM precipitation, as well as vertical velocity and divergence data from NCEP analyses, with a focus on South America. We find that enhanced CO observed by MLS is a good proxy of aerosols during the dry, biomass burning season (June–October), while it may be not appropriate to equate CO and aerosol during the wet rainy season as the aerosol loading is much lower and CO can still be quite high. We find evidence of suppressed precipitation and reduced ice particle radii associated with polluted clouds, compared to that for clean clouds, for both dry and wet seasons, although more distinctly in the dry season. The dynamical conditions, as indicated by the large-scale vertical velocity at 500 hPa and horizontal divergence at 850 hPa, can not explain the precipitation differences for the polluted and clean clouds, suggesting that aerosol-cloud-precipitation interactions may play a dominant role in contributing to the suppressed rainfall when aerosol is abundant. The difference in precipitation between polluted and clean clouds is weaker in the wet season than in the dry season and could be due to the different large-scale conditions (such as boundary layer humidity) and different aerosol concentrations in the two seasons.

[17] This study is our first attempt to quantify the relationships among aerosol, ice cloud and precipitation. Exact physical mechanisms that contribute to these relationships require detailed cloud-resolving modeling studies and further analysis using height-resolved tropospheric cloud profiles (such as from CloudSat/CALIPSO). We are hopeful that the availability of more satellite observations will help to narrow down the uncertainties of aerosol effects in climate model simulations and predictions.

[18] **Acknowledgments.** We thank support from the NASA Atmospheric Chemistry Modeling and Analysis Program and NASA Interdisciplinary Research in Earth Science. The Caltech Jet Propulsion Laboratory is supported by NASA. The National Center for Atmospheric Research is sponsored by the National Science Foundation.

References

Albrecht, B. A. (1989), Aerosols, cloud microphysics, and fractional cloudiness, *Science*, *245*, 1227–1230.

Andreae, M. O., D. Rosenfeld, P. Artaxo, A. A. Costa, G. P. Frank, K. M. Longo, and M. A. F. Silva-Dias (2004), Smoking rain clouds over the Amazon, *Science*, *303*, 1337–1342, doi:10.1126/science.1092779.

Artaxo, P., J. V. Martins, M. A. Yamasoe, A. S. Procópio, T. M. Pauliquevis, M. O. Andreae, P. Guyon, L. V. Gatti, and A. M. C. Leal (2002), Physical and chemical properties of aerosols in the wet and dry seasons in Rondônia, Amazonia, *J. Geophys. Res.*, *107*(D20), 8081, doi:10.1029/2001JD000666.

Chylek, P., M. K. Dubey, U. Lohmann, V. Ramanathan, Y. J. Kaufman, G. Lesins, J. Hudson, G. Altmann, and S. Olsen (2006), Aerosol indirect effect over the Indian Ocean, *Geophys. Res. Lett.*, *33*, L06806, doi:10.1029/2005GL025397.

Coakley, J. A., and C. D. Walsh (2002), Limits to the aerosol indirect radiative effect derived from observations of ship tracks, *J. Atmos. Sci.*, *59*, 668–680.

Facchini, M. C., et al. (1999), Cloud albedo enhancement by surface-active organic solutes in growing droplets, *Nature*, *401*, 257–259.

Folkins, I., and R. V. Martin (2005), The vertical structure of tropical convection, its impact on the budgets of water vapor and ozone, *J. Atmos. Sci.*, *62*, 1560–1573.

Huffman, G. J., et al. (2001), Global precipitation at one-degree daily resolution from multi-satellite observations, *J. Hydrometeorol.*, *2*(1), 36–50.

Intergovernmental Panel on Climate Change (2007), *Climate Change 2007: The Physical Science Basis. Contribution of Working Group I to the Fourth Assessment Report of the Intergovernmental Panel on Climate Change*, Cambridge Univ. Press, Cambridge, U. K.

Kaufman, Y. J., and R. S. Fraser (1997), The effect of smoke particles on clouds and climate forcing, *Science*, *277*, 1636–1639.

Kaufman, Y. J., D. Tanré, L. A. Remer, E. F. Vermote, A. Chu, and B. N. Holben (1997), Operational remote sensing of tropospheric aerosol over land from EOS moderate resolution imaging spectroradiometer, *J. Geophys. Res.*, *102*, 17,051–17,067.

Jiang, J. H., N. J. Livesey, H. Su, L. Neary, J. C. McConnell, and N. A. D. Richards (2007), Connecting surface emissions, convective uplifting, and long-range transport of carbon monoxide in the upper troposphere: New observations from the Aura Microwave Limb Sounder, *Geophys. Res. Lett.*, *34*, L18812, doi:10.1029/2007GL030638.

Lin, J. C., T. Matsui, R. A. Pielke Sr., and C. Kummerow (2006), Effects of biomass-burning-derived aerosols on precipitation and clouds in the Amazon Basin: A satellite-based empirical study, *J. Geophys. Res.*, *111*, D19204, doi:10.1029/2005JD006884.

Livesey, N. J., et al. (2008), Validation of Aura Microwave Limb Sounder O_3 and CO observations in the upper troposphere and lower stratosphere, *J. Geophys. Res.*, *113*, D15S02, doi:10.1029/2007JD008805.

Lohmann, U., and J. Feichter (2005), Global indirect aerosol effects: A review, *Atmos. Chem. Phys.*, *4*, 7561–7614.

Massie, S. T., A. Heymsfield, C. Schmitt, D. Müller, and P. Seifert (2007), Aerosol indirect effects as a function of cloud top pressure, *J. Geophys. Res.*, *112*, D06202, doi:10.1029/2006JD007383.

Matheson, M. A., J. A. Coakley Jr., and W. R. Tahnk (2005), Aerosol and cloud property relationships for summertime stratiform clouds in the northeastern Atlantic from Advanced Very High Resolution Radiometer observations, *J. Geophys. Res.*, *110*, D24204, doi:10.1029/2005JD006165.

Nakajima, T., and M. D. King (1990), Determination of the optical thickness and effective particle radius of clouds from reflected solar radiation measurements. Part I: Theory, *J. Atmos. Sci.*, *47*, 1878–1893.

Nakajima, T., A. Higurashi, K. Kawamoto, and J. E. Penner (2001), A possible correlation between satellite-derived cloud and aerosol microphysical parameters, *Geophys. Res. Lett.*, *28*, 1171–1174.

Penner, J. E., et al. (2001), Aerosols, their direct and indirect effects, in *Climate Change 2001: The Scientific Basis. Contribution of Working Group I to the Third Assessment Report of the Intergovernmental Panel on Climate Change*, edited by J. T. Houghton et al., pp. 289–348, Cambridge Univ. Press, New York.

Platnick, S., et al. (2003), The MODIS cloud products: Algorithms and examples from terra, *IEEE Trans. Geosci. Remote Sens.*, *41*, 459–473.

Ramanathan, V., et al. (2001), Aerosols, climate, and the hydrological cycle, *Science*, *294*, 2119–2124.

Remer, L. A., et al. (2005), The MODIS aerosol algorithm, products and validation, *J. Atmos. Sci.*, *62*, 947–973.

Rosenfeld, D. (1999), TRMM observed first direct evidence of smoke from forest fires inhibiting rainfall, *Geophys. Res. Lett.*, *26*, 3105–3108.

Schoeberl, M. R., and S. Talabac (2007), The sensor web: A future technique for science return, in *Observing Systems for Atmospheric Composition: Satellite, Aircraft Sensor Web and Ground-Base Observational Methods and Strategies*, edited by G. Visconti et al., pp. 203–206, Springer, New York.

Sekiguchi, M., T. Nakajima, K. Suzuki, K. Kawamoto, A. Higurashi, D. Rosenfeld, I. Sano, and S. Mukai (2003), A study of the direct and indirect effects of aerosols using global satellite data sets of aerosol and cloud parameters, *J. Geophys. Res.*, *108*(D22), 4699, doi:10.1029/2002JD003359.

Sherwood, S. (2002), Aerosols and ice particle size in tropical cumulonimbus, *J. Clim.*, *15*, 1051–1063.

Twomey, S. (1977), *Atmospheric Aerosols*, 302 pp., Elsevier Sci., Amsterdam.

Twomey, S., M. Piepgrass, and T. L. Wolfe (1984), An assessment of the impact of pollution of global cloud albedo, *Tellus, Ser. B*, *36*, 356–366.

Wu, D. L., J. H. Jiang, W. G. Read, R. T. Austin, C. P. Davis, A. Lambert, G. L. Stephens, D. G. Vane, and J. W. Waters (2008), Validation of the

Aura MLS cloud ice water content measurements, *J. Geophys. Res.*, *113*, D15S10, doi:10.1029/2007JD008931.

P. Colarco, NASA Goddard Space Flight Center, Mail Code 916, Greenbelt, MD 20771, USA.

J. H. Jiang, N. J. Livesey, and H. Su, Jet Propulsion Laboratory, California Institute of Technology, Mail Stop 183-701, 4800 Oak Grove Drive, Pasadena, CA 91109, USA. (jonathan.h.jiang@jpl.nasa.gov)

S. T. Massie, Atmospheric Chemistry Division, National Center for Atmospheric Research, P.O. Box 3000, Boulder, CO 80307, USA.

S. Platnick, Climate and Radiation Branch, NASA Goddard Space Flight Center, Mail Code 913, Greenbelt, MD 20771, USA.

M. R. Schoeberl, NASA Goddard Space Flight Center, Mail Code 910, Greenbelt, MD 20771, USA.